

Local Phase Velocity Imaging (LPVI) as a New Technique for Shear Wave Elastography

Matthew W. Urban¹; Piotr Kijanka^{1,2}

¹Department of Radiology, Mayo Clinic, Rochester, MN, USA

²Department of Robotics and Mechatronics, AGH University of Science and Technology, Krakow, Poland

ABSTRACT

Shear wave elastography is used in many clinical settings to measure the mechanical properties of soft tissues such as the liver, kidney, breast, and thyroid. In most implementations, the shear wave group velocity is measured using time-of-flight methods in the time-domain. However, different factors related to the estimation of the group velocity can cause variation in the results. Factors such as acquisition parameters, processing, tissue inhomogeneities and viscoelasticity can cause these variations. We propose to use methods that rely on phase velocities, shear wave velocities at specific frequencies, to standardize measurements across different clinical applications. We have developed methods for creating maps of phase velocity using Local Phase Velocity Imaging (LPVI). The LPVI method involves directional and wavenumber filtering before applying various steps of Fourier-based operations to obtain localized maps of phase velocity over large bandwidths. We will demonstrate how LPVI works in numerical data, tissue mimicking phantoms, and *in vivo* liver tissue. The LPVI method has enormous potential because the frequency, for which the phase velocity maps are reconstructed, can be controlled, optimized, and standardized for a wide array of clinical applications.

Keywords: Ultrasound, shear wave elastography, phase velocity, inclusion, viscoelasticity.

1. INTRODUCTION

Shear wave elastography (SWE) is increasingly being used for multiple clinical applications (1-3). Typically, a focused ultrasound “push” beam to create acoustic radiation force (ARF) is used to generate propagating shear waves. Ultrafast ultrasound imaging techniques are used for tracking the propagation of the shear waves. Time-of-flight (TOF) algorithms are used to measure the group velocity, or propagation velocity of the time-domain wave packet. The group velocity or Young’s modulus is typically reported in clinical implementations of SWE (2).

Generally, an assumption is made that the tissue is linear, elastic, homogeneous, isotropic, and incompressible. However, soft tissues are inherently viscoelastic and the frequency content of the wave can affect the group velocity estimate. As an alternative, the phase velocity, or wave velocity at a particular frequency, can be estimated. If a certain frequency or set of frequencies were used for an application, this could provide a level of standardization that may not be present in the case of using group velocity estimates.

Multiple methods have been employed for generating two-dimensional (2D) images of the group velocity (4-7) using different TOF algorithms. Recently, several groups have pursued creating 2D images of phase velocity. Budelli, *et al.*, reported a method that used a sliding window to compute the phase gradient (8). Additionally, we developed a method called local phase velocity imaging (LPVI), which is described in detail in this paper (9). The LPVI method uses a sliding window and Fourier techniques, as well as, directional and wavenumber filtering to recover local estimates of phase velocities at specified frequencies or bands of frequencies. Examples of the uses of LPVI in phantoms and *in vivo* tissue will be shown.

¹ urban.matthew@mayo.edu

² kijanka.piotr@mayo.edu; piotr.kijanka@agh.edu.pl

2. METHODS

2.1 Description of LPVI

A block diagram for the LPVI reconstruction is shown in Fig. 1. The three-dimensional (3D) shear wave data $v(z,x,t)$ is acquired after an acoustic radiation force push and ultrasound acquisition of data for estimating the wave motion. The data is transformed into a Fourier domain with dimensions (kz,kx,f) for the purposes of applying directional and bandpass wavenumber filters. The directional filter will typically isolate waves that are traveling left-to-right (LR) or right-to-left (RL). The wavenumber filter can be applied to limit waves traveling over a certain range of wave velocities such as from 0.5-10.0 m/s. After applying the filters, the inverse Fourier transform is applied to return to the spatiotemporal domain. The next step is to apply a one-dimensional (1D) Fourier transform and select a frequency of interest, f_0 . Once the frequency of interest is identified, a sliding window, $W_{x,z}$, is applied. A 2D spatial Fourier transform is applied for each set of windowed data and the dominant wavenumber is identified. This wavenumber is used for the calculation of the phase velocity for that spatial window. As the spatial window is applied over the whole imaging plane, the aforementioned steps of calculating the 2D spatial Fourier transform and phase velocity calculation are performed until the whole image is reconstructed. For more details, the reader is referred to (9). This process is completed for data acquired with an ARF push to the left of the region-of-interest (ROI) and another to the right of the ROI, and the two reconstructions are averaged.

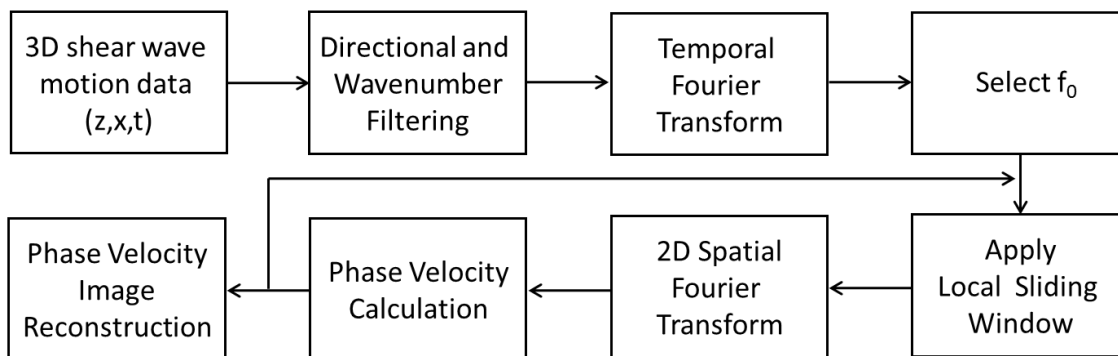


Figure 1 – Block diagram for LPVI image reconstruction.

2.2 Phantom Experiments

The LPVI method was tested on data sets acquired from imaging phantoms. The data was acquired using a Verasonics system (V1, Verasonics, Kirkland, WA) equipped with a L7-4 linear array transducer (Philips Healthcare, Andover, MA). An ARF push beam was used to generate shear waves, and angular plane wave compounding was used for the motion tracking acquisition (10). Motion was estimated using an autocorrelation algorithm (11).

Figure 2 shows the results in two elastic homogeneous phantoms (Model 039, CIRS, Inc., Norfolk, VA) at various frequencies. The results are relatively uniform and constant across frequency. Figure 3 shows results from Type IV inclusions with diameter of 6.49 mm with Young's modulus of $E = 80$ kPa in a background of $E = 25$ kPa (Model 049A, CIRS, Inc., Norfolk, VA) over a series of sliding windows, $W_{x,z}$, for $f_0 = 947$ Hz. As the window size increases, the edge of the reconstructed inclusion becomes smoother.

Figure 4 shows the results in the inclusion phantom with a window of 4.0 x 4.0 mm for various frequencies. The shape of the inclusion becomes more circular as the frequency increases, and the average value increases as well. Figure 5 shows the LPVI reconstructions for inclusions of different size at $f_0 = 1000$ Hz. The inclusions have good contrast down to a diameter of 4.05 mm while the inclusion with a diameter of 2.53 mm is not well visualized.

Figure 6 shows LPVI reconstructions from custom made homogeneous viscoelastic phantoms (CIRS, Inc., Norfolk, VA). In the viscoelastic media, the phase velocity is fairly uniform and varies as a function of frequency.

Figure 7 shows the results from a simulation model with a background modulus $E = 7.84$ kPa, and inclusions with $E = 25$ and 3.24 kPa, for the top and bottom inclusions, respectively. Each

reconstruction used a different combination of motion (particle displacement or velocity), use of directional and wavenumber filters, and the use of individual ARF push beams or simultaneous use of ARF push beams. The reconstructions using the particle velocity and directional and wavenumber filters were the best reconstructions. The particle displacement at higher frequencies did not provide valid reconstructions.

2.3 *In Vivo* Liver Experiments

Measurements were made in the liver of a healthy human subject. The experiment protocol was approved by the Mayo Clinic Institutional Review Board and written informed consent was obtained prior to scanning. Under the guidance of B-mode imaging, a trained sonographer located a region of interest within the liver. A Verasonics Vantage system (Verasonics, Inc., Kirkland, WA) was used with a C5-2v transducer (Verasonics, Inc., Kirkland, WA). To produce shear waves, a single focused push beam with push duration of 600 μ s was transmitted. The motion tracking was performed using wide beams with an $f/9.9$ focal configuration transmitted with a frequency of 2 MHz. Received signals from two steering angles were compounded (10), giving an effective pulse repetition frequency of 2.77 kHz.

3. RESULTS

3.1 Phantom Experiments

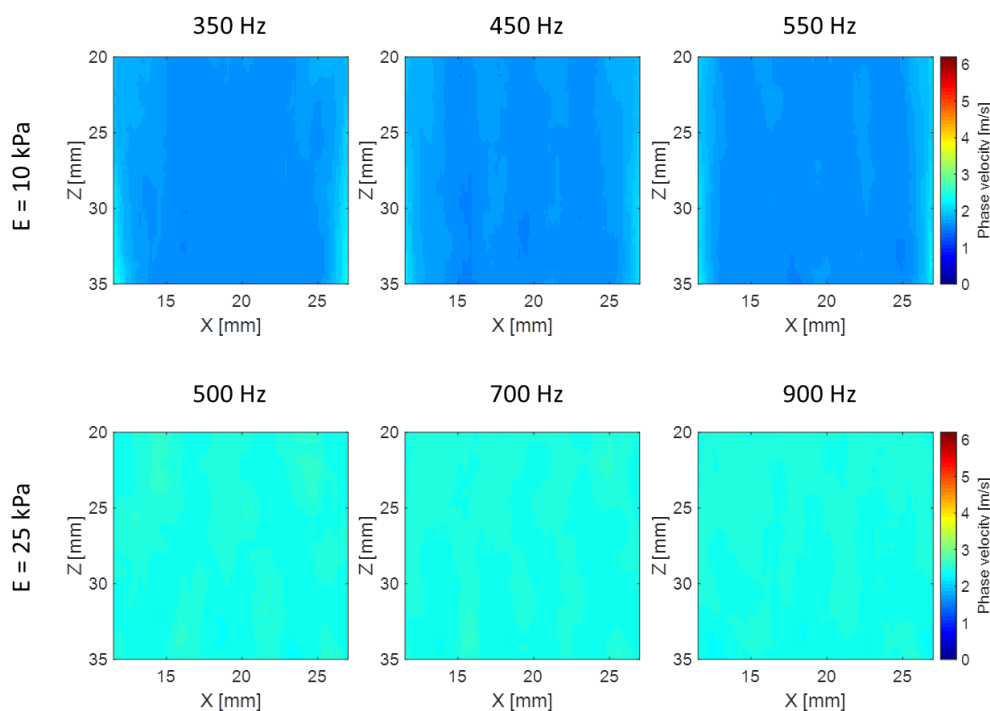


Figure 2 – LPVI results in elastic homogeneous phantoms with a sliding window of $W_{x,z} = 4.0 \times 4.0$ mm. Top row: Phantom with $E = 10$ kPa with reconstructions at $f_0 = 350, 450,$ and 550 Hz. Bottom row: Phantom with $E = 25$ kPa with reconstructions at $f_0 = 500, 700,$ and 900 Hz.

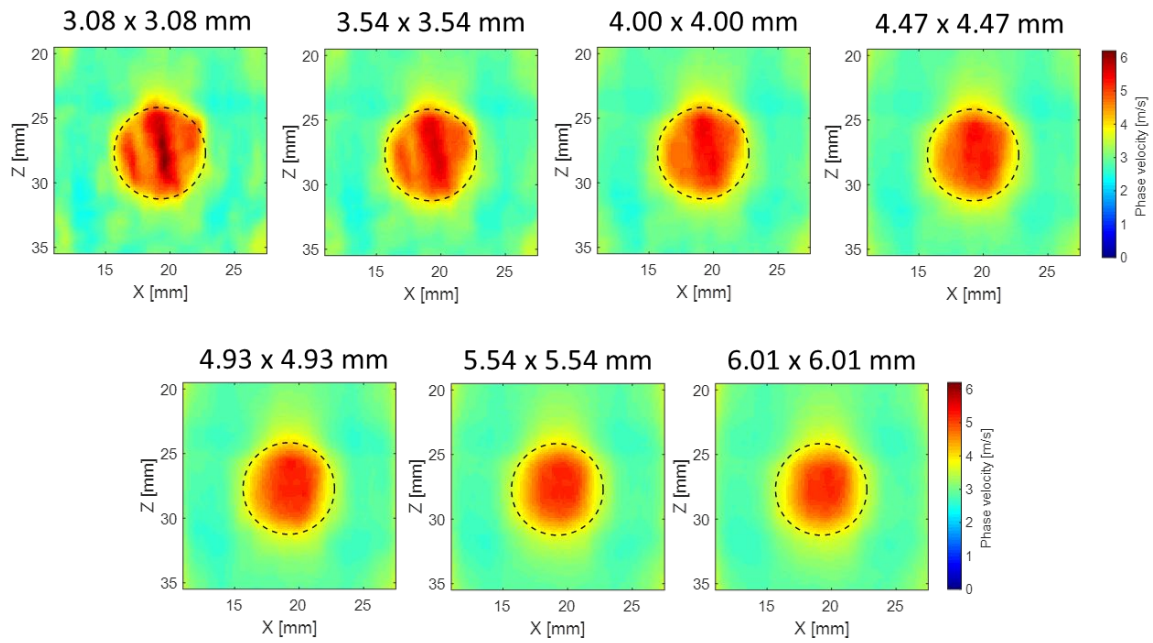


Figure 3 – LPVI results in elastic phantom with a cylindrical inclusion at $f_0 = 947$ Hz with different sliding windows.

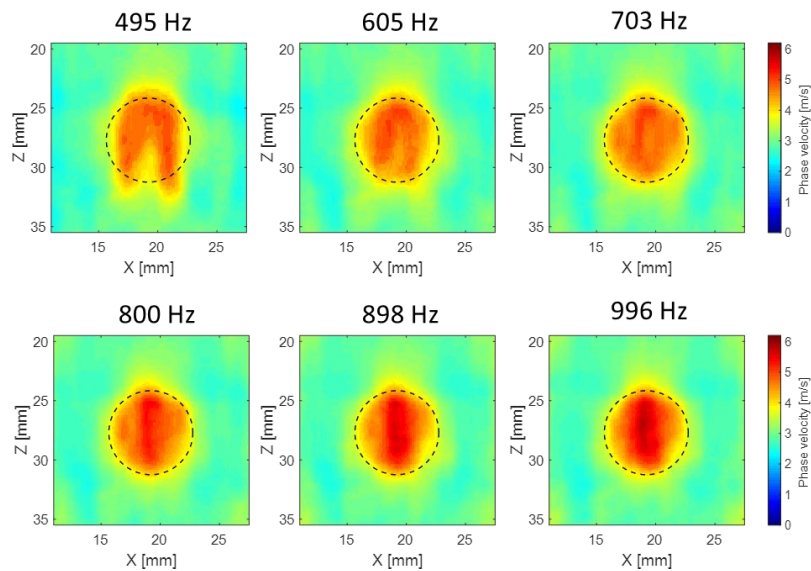


Figure 4 – LPVI results in elastic phantom with a cylindrical inclusion with $W_{x,z} = 4.0 \times 4.0$ mm and varying frequencies.

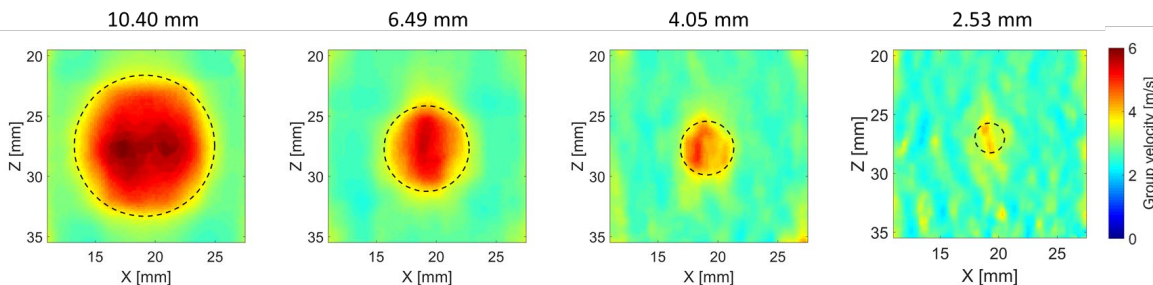


Figure 5 – LPVI results in elastic phantom with cylindrical inclusions of varying size at a frequency of 1000 Hz.

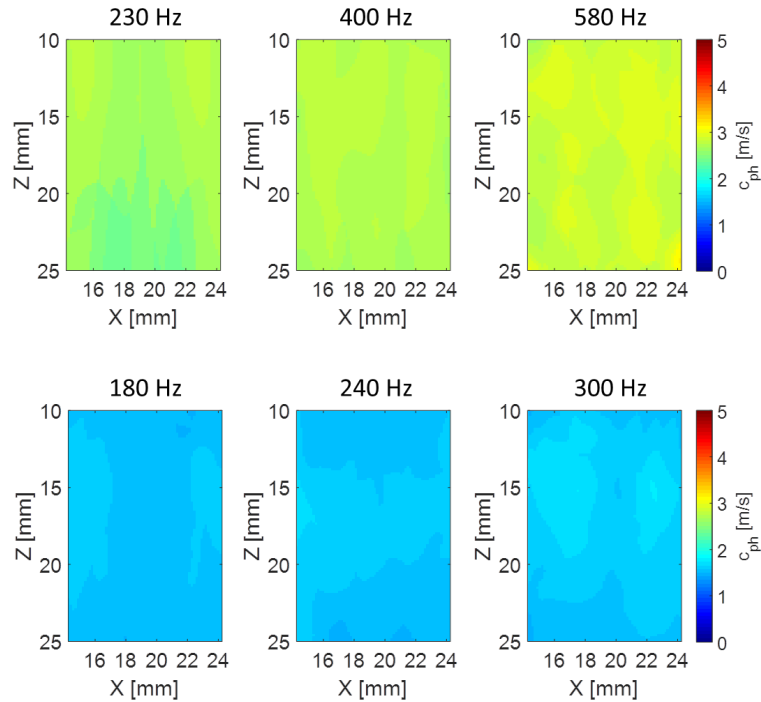


Figure 6 – LPVI results in viscoelastic homogeneous phantoms with varying frequencies.

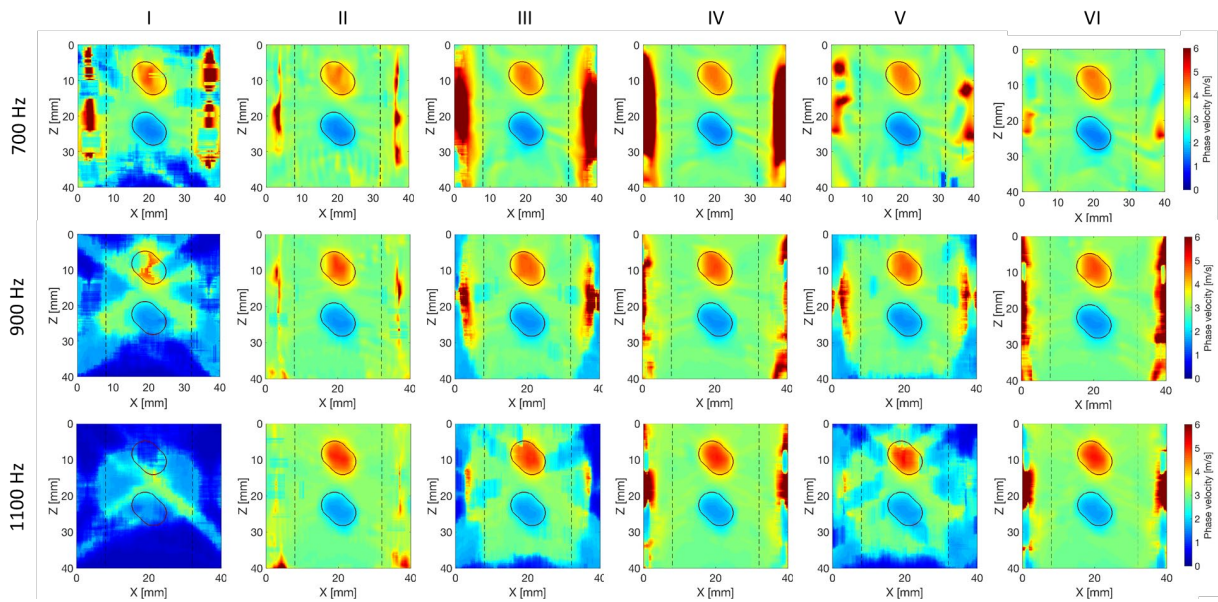


Figure 7 – LPVI results in simulated elastic phantom with inclusions processed with different shear wave motion and filtering. I. particle displacement signal as an input signal, with inactive directional and wavenumber filters, for a single ultrasound focused push beam; II. particle velocity signal as an input signal, with inactive directional and wavenumber filters, for a single ultrasound focused push beam; III. particle displacement signal as an input signal, with active directional and wavenumber filters, for a single ultrasound focused push beam; IV. particle velocity signal as an input signal, with active directional and wavenumber filters, for a single ultrasound focused push beam; V. particle displacement signal as an input signal, with active directional and wavenumber filters, for multiple ultrasound focused push beams; VI. particle velocity signal as an input signal, with active directional and wavenumber filters, for multiple ultrasound focused push beams. Vertical, dashed lines separate regions where the focused ultrasound push beams were located.

3.2 *In Vivo* Liver Experiments

Figure 8 shows the results from *in vivo* liver at 90, 130, and 170 Hz. The phase velocity increases

with frequency and the maps are generally uniform with ROIs of size 10 x 7 mm. The ROI is smaller in the liver compared to the purely elastic materials due to the shear wave attenuation associated with viscoelastic materials.

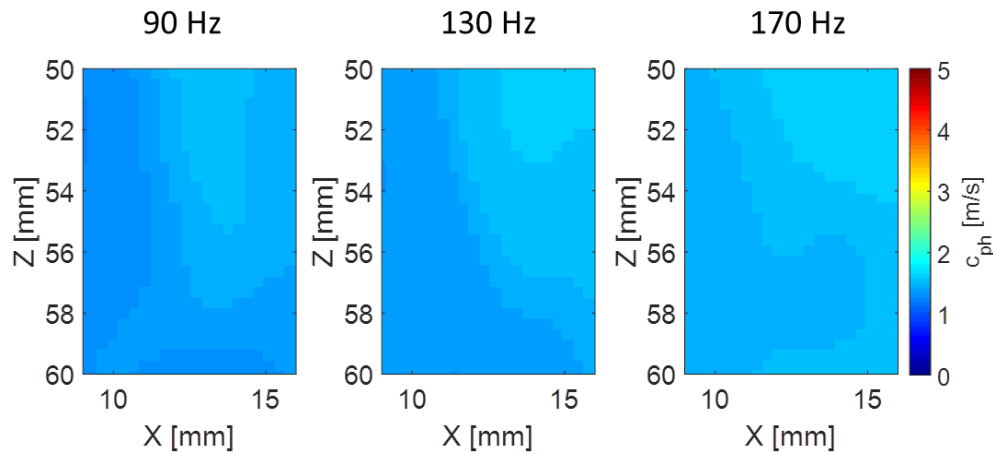


Figure 8 – LPVI results in *in vivo* liver tissue with varying frequencies.

4. DISCUSSION

We presented a new method called local phase velocity imaging. This method has been extensively tested in phantoms and we have explored how different parameters are related to how the reconstruction affects the resulting images. Among these parameters are the window size, the frequency of interest, and motion type, and the use of directional and wavenumber filters.

The LPVI method produces very uniform reconstructions in homogeneous media as demonstrated in Figs. 2, 6, and 8. The ROI size can be larger in materials that more elastic compared to viscoelastic materials. In the viscoelastic material, the shear wave attenuates with distance and reduces the effective ROI size.

There is a trade-off when choosing the window size. With smaller windows, the transition zone is shorter from the inclusion to the background, but there is more variation in the inclusion and background. With a larger window, the variation is reduced substantially, but the transition is increased. As the frequency increases, the transition from the inclusion to the background is sharper. Additionally, as the frequency increases, the mean value of the inclusion increases.

We have generally used the particle velocity to perform the reconstructions with LPVI as the frequency content of the shear waves covers a larger bandwidth as compared to the particle displacement. However, as demonstrated in Fig. 7, the displacement can be used reliably if appropriate directional and wavenumber filters are employed.

Also, in Fig. 7, we demonstrated that using two separate ARF pushes or one simultaneous push with two ARF push beams, we can reconstruct similar images. This is advantageous for saving time in the acquisition as is done with the comb push ultrasound shear elastography (CUSE) method (6, 12).

In the future, we need to evaluate using the LPVI method for *in vivo* use in homogeneous or heterogeneous tissues. There is a large potential for standardizing reconstructions to a particular frequency for different applications for optimal separation of normal versus abnormal tissue.

The frequencies that have been used in some of the elastic reconstructions are high for most SWE applications, >500 Hz. To produce shear waves with broad frequency content, we will also explore ways to optimize the ARF pushes including the shape and duration.

5. CONCLUSIONS

The local phase velocity imaging method is a robust approach for reconstructing images of phase velocity. We have demonstrated reconstructions in homogeneous elastic and viscoelastic materials. In addition, we have reconstructed images in elastic phantoms with simulated inclusions. We have tested multiple parameters related to the LPVI reconstructions including the sliding window size, the frequency of interest, the type of shear wave motion used, the used of directional and wavenumber filters, and the type of ARF excitation that is employed. Optimal imaging is performed with the use of particle velocity with directional and wavenumber filters. Future work will be devoted towards optimizations for specific *in vivo* applications.

ACKNOWLEDGEMENTS

This work was supported in part by grant R01DK092255 from the National Institutes of Health and in part from Mayo Clinic Research Committee. The content is solely the responsibility of authors and does not necessarily represent the official views of the National Institute of Diabetes and Digestive and Kidney Diseases or the National Institutes of Health.

REFERENCES

1. Sarvazyan A, Hall TJ, Urban MW, Fatemi M, Aglyamov SR, Garra B. Elasticity imaging - an emerging branch of medical imaging. An overview. *Curr Med Imaging Rev.* 2011;7(4):255-82.
2. Bamber J, Cosgrove D, Dietrich CF, Fromageau J, Bojunga J, Calliada F, et al. EFSUMB guidelines and recommendations on the clinical use of ultrasound elastography. part 1: basic principles and technology. *Ultraschall in Med.* 2013;34(02):169-84.
3. Cosgrove D, Piscaglia F, Bamber J, Bojunga J, Correas JM, Gilja OH, et al. EFSUMB guidelines and recommendations on the clinical use of ultrasound elastography. part 2: clinical applications. *Ultraschall in Med.* 2013;34(03):238-53.
4. Bercoff J, Tanter M, Fink M. Supersonic shear imaging: a new technique for soft tissue elasticity mapping. *IEEE Trans Ultrason Ferroelectr Freq Control.* 2004;51(4):396-409.
5. Rouze NC, Wang MH, Palmeri ML, Nightingale KR. Parameters affecting the resolution and accuracy of 2-D quantitative shear wave images. *IEEE Trans Ultrasonics Ferroelectr Freq Control.* 2012;59(8):1729-40.
6. Song P, Zhao H, Manduca A, Urban MW, Greenleaf JF, Chen S. Comb-push ultrasound shear elastography (CUSE): a novel method for two-dimensional shear elasticity imaging of soft tissues. *Ieee T Med Imaging.* 2012;31(9):1821-32.
7. Song P, Manduca A, Zhao H, Urban MW, Greenleaf JF, Chen S. Fast shear compounding using robust 2-D shear wave speed calculation and multi-directional filtering. *Ultrasound in Medicine & Biology.* 2014;40(6):1343-55.
8. Budelli E, Brum J, Bernal M, Deffieux T, Tanter M, Lerna P, et al. A diffraction correction for storage and loss moduli imaging using radiation force based elastography. *Physics in Medicine and Biology.* 2017;62(1):91-106.
9. Kijanka P, Urban MW. Local phase velocity based imaging (LPVI): a new technique used for ultrasound shear wave elastography. *Ieee T Med Imaging.* 2018;38(4):894-908.
10. Montaldo G, Tanter M, Bercoff J, Benech N, Fink M. Coherent plane-wave compounding for very high frame rate ultrasonography and transient elastography. *IEEE Trans Ultrason Ferroelectr Freq Control.* 2009;56(3):489-506.
11. Kasai C, Namekawa K, Koyano A, Omoto R. Real-time two-dimensional blood flow imaging using an autocorrelation technique. *IEEE Trans Sonics and Ultrasonics.* 1985;SU-32(3):458-64.
12. Song P, Urban MW, Manduca A, Zhao H, Greenleaf JF, Chen S. Comb-push ultrasound shear elastography (CUSE) with various ultrasound push beams. *Ieee T Med Imaging.* 2013;32(8):1435-47.